Article

Discovery Medicine 2025; 37(192): 152–165
https://doi.org/10.24976/Discov.Med.202537192.13

Zinc Finger SWIM-Type Containing 3 Reprograms Lipid Metabolism and Drives Breast Cancer Progression

Xiao Ma[1,†], Ancai Wang[2,†], Yu Wang[1], Jintao Ma[1], Yunchong Liu[1,*], Yu Mei[1,*]

[1]Breast Surgery, Jinan Maternity and Child Care Hospital Affiliated to Shandong First Medical University, 250001 Jinan, Shandong, China
[2]Department of Chest, Heart, Thyroid and Breast Surgery, Rongcheng People's Hospital, 264300 Rongcheng, Shandong, China
*Correspondence: shamo-ak@163.com (Yunchong Liu); may_chch@163.com (Yu Mei)
[†]These authors contributed equally.
Published: 20 January 2025

Background: Zinc finger proteins (ZNFs) have been proved to play important roles in driving the progression of breast cancer (BC), one of the most common cancers among women. This study aimed to investigate the involvement of zinc-finger SWIM domain-containing protein 3 (*ZSWIM3*) in promoting BC cell progression by regulating lipid metabolism.

Methods: Differential expression of *ZSWIM3* in BC was confirmed by comparing its expression in normal human mammary epithelial cells and BC cells. MCF7 cells, a BC cell line, were subjected to *ZSWIM3* knockdown/overexpression experiments. The lipid contents in MCF7 cells were measured by assay kits and immunofluorescence test. The lipogenic enzymes in the cells were detected by enzyme-linked immunosorbent assay (ELISA). The cells were also subjected to further transfection experiments to manipulate the expression of sterol regulatory element-binding transcription factor 1 (*SREBF1*)/*SREBF2* in *ZSWIM3*-regulated MCF7 cells to verify whether the *ZSWIM3* targets *SREBF1/SREBF2*. Subsequently, the lipid contents in the transfected cells were determined, and the cell viability, proliferation and metastasis were measured.

Results: *ZSWIM3* was overexpressed in BC cells. *ZSWIM3* knockdown/overexpression led to a significant decrease/increase of the lipid contents including triglyceride, free fatty acid, cholesterol, phospholipid and neutral lipid, and lipogenic enzymes ($p < 0.01$). The *ZSWIM3* knockdown decreased the expression of *SREBF1* and *SREBF2* ($p < 0.01$). Our findings showed that lipid content reduction induced by *ZSWIM3* knockdown was reversed by *SREBF1/SREBF2* overexpression. MCF7 cell viability, proliferation and metastasis, which were all suppressed by *ZSWIM3* knockdown ($p < 0.001$), were reversible through *SREBF1/SREBF2* overexpression ($p < 0.001$). On the other hand, the *ZSWIM3* overexpression increased *SREBF1* and *SREBF2* expression ($p < 0.001$). Lipid content elevation, as well as increased MCF7 cell viability, proliferation and metastasis, which were induced by *ZSWIM3* overexpression, could be counteracted by *SREBF1/SREBF2* downregulation ($p < 0.001$).

Conclusion: *ZSWIM3* promotes BC progression by enhancing lipid synthesis. This study reveals the malevolent effect of *ZSWIM3* on BC, underpinned by the reprogramming of lipid metabolism, providing insights into potential therapeutic targets for BC treatments.

Keywords: breast cancer; *ZSWIM3*; lipid metabolism; *SREBF1*; *SREBF2*

Introduction

Breast cancer (BC) is responsible for the highest cancer-related mortality in the female population [1]. It has been reported that BC causes approximately 42,000 deaths in women every year, and in the year 2020, about 2.3 million women were diagnosed with BC and 68,500 succumbed to BC [2,3]. At present, there is no effective cure for treating BC, but molecular studies have enabled us to acquire a profound understanding of how molecules and cellular pathways mediate BC progression, which is instrumental in advancing the development of both diagnostic markers and therapeutic targets [4,5]. Nonetheless, to accelerate the identification of novel targets and potential therapeutic strategies, a more extensive exploration of the molecular mechanisms underlying BC progression is required.

Metabolic patterns of cancer cells are altered to cater to the changing energy requirements and maintenance needs of malignancy, and thus, reprogrammed metabolisms, including reprogrammed lipid metabolism, represent the hallmarks of cancer [6]. Studies have claimed that increased synthesis or biosynthesis of *de novo* fatty acid [7,8] and cholesterol [9,10] could promote tumor progression by building cell blocks, providing energy sources and regulating gene expression as well as signaling pathways. It is noteworthy that the altered lipid metabolism can impact tumorigenesis and immune evasion in BC [11] and that the BC cells can be protected from ferroptosis by adipocytes [12]. In order to facilitate the development of more effective BC treatment, further intricate mechanisms linking lipid metabolism with BC progression need to be unraveled.

The zinc finger is a short finger-like conformation in proteins containing zinc ions, and the zinc finger proteins (ZNFs) have been identified in various organisms and are associated with gene expression, cell progression and other biological processes [13,14]. The zinc finger SWItch/sucrose non-fermentable 2 (SWI2/SNF2) and Mutator/DRifter (MuDR) (SWIM) domain, while being evolutionally conserved in many organisms, remains an uncharacterized domain of zinc finger [15]. A variety of ZNFs have been proven to play roles in BC progression and even identified as oncogenic biomarkers for BC [16–18], whereas the functions of zinc-finger SWIM domain-containing protein family (ZSWIM) in BC remain unclear. Among all the ZSWIM proteins, the ZSWIM3 was found to function through DNA-binding and protein-binding interactions, and might interact with cancer-related tumor necrosis factor receptor-associated factor 2 (TRAF2) and nuclear transcription factor kappa B (NF-κB) pathway [19]. Sterol regulatory element-binding proteins (SREBPs), particularly SREBP1 and SREBP2, are master regulators of lipid metabolism [20], orchestrating fatty acid and cholesterol synthesis pathways [21,22]. Our study delves into the role of ZSWIM3 in breast cancer progression and its interaction with lipid metabolism pathways mediated by SREBP1 and SREBP2. We aimed to elucidate how ZSWIM3 controls SREBP1 and SREBP2 expression in the process of influencing BC progression.

In the present study, we investigated the role of lipid metabolism reprogramming underlying the effects of ZSWIM3 on BC progression by adopting an *in vitro* experimental design. In this study, we shed light on a novel mechanism through which ZSWIM3 influences BC development and offer a new perspective on therapeutic avenues for treating BC.

Materials and Methods

Cell Culture

The normal human mammary epithelial cells MCF10A (iCell-h131) and human breast cancer cells MCF7 (iCell-h129), ZR-75-1 (iCell-h288), MDA-MB-231 (iCell-h133) and HS578T (iCell-h105) were obtained from iCell Bioscience Inc. (Shanghai, China). The Dulbecco's Modified Eagle Medium (DMEM; iCell-0001, iCell Bioscience Inc., Shanghai, China) supplemented with 10% fetal bovine serum (FBS; iCell-0500, iCell Bioscience Inc., Shanghai, China) was used as the culture medium. During cell culture, the antibiotics (Penicillin and Streptomycin) (1%; iCell-15140-122, iCell Bioscience Inc., Shanghai, China) were added into the medium. The cells were cultured at 37 °C, under the atmosphere of 5% CO_2 and 70–80% humidity. All cell lines were authenticated by short tandem repeat (STR) test and were tested by mycoplasma test.

Cell Transfection

Cell transfection was conducted using Lipofectamine™ 3000 (L3000001, Invitrogen, Carlsbad, CA, USA) to manipulate gene expression in MCF7 cells. To induce gene knockdown, small hairpin (sh)RNAs targeting *ZSWIM3* (sh-*ZSWIM3*; 5′-CACCGCATCGTAGTTCAGCAAATCCCGAAGGATTTGCTGAACTACGATGC-3′), sterol regulatory element-binding transcription factor 1 (*SREBF1*) (sh-*SREBF1*; 5′-CACCGCTTTCTGCAACACAGCAACCCGAAGGTTGCTGTGTTGCAGAAAGC-3′), *SREBF2* (sh-*SREBF2*; 5′-CACCGCCATTCTGACCACAATGCCTGTAATCGAAATTACAGGCATTGTGGTCAGAATGG-3′) and the negative control (sh-NC; 5′-CACCGCCAAGTCCACCGTAAGTCCTTTAATCGAAATTAAAGGACTTACGGTGGACTTGG-3′) were inserted into pcDNA 3.1 vector. To induce overexpression, pcDNA 3.1 vector was inserted with the open reading frame of *ZSWIM3* (OE-*ZSWIM3*; Gene ID: 140831), *SREBF1* (OE-*SREBF1*; Gene ID: 6720), *SREBF2* (OE-*SREBF2*; Gene ID: 6721) or the blank vector (OE-NC) were used for transfection. All vectors were constructed by GeneChem (Shanghai, China).

Real-Time Reverse-Transcription Polymerase Chain Reaction (RT-qPCR)

Total RNA was extracted using TRNzol Universal RNA extraction kit (DP424, Tiangen, Beijing, China) and reverse-transcribed into cDNA using cDNA Reverse Transcription Kit (4368814, Applied Biosystems Inc., Carlsbad, CA, USA). RT-qPCR reaction was performed according to the instruction of PowerUp™ SYBR™ Green premix (A25742, Applied Biosystems Inc., Carlsbad, CA, USA). The gene expression data were analyzed by the $2^{-\Delta\Delta Ct}$ method. Primers utilized in this experiment include: *ZSWIM3* (forward 5′-GCTTCAGCGCCTACAAAAGG3′, reverse 5′-TGGAGTGAAAGTGGAGTGGG-3′), *SREBF1* (forward 5′-GGCATGGACGGGTACATCTT-3′, reverse 5′-GTGTGCCAACAAGGGTTGTG-3′), *SREBF2* (forward 5′-TTCCGATGTACACATGGCGT-3′, reverse 5′-GTGTGCTCGGTGGGATCTTC-3′) and glyceraldehyde-3-phosphate dehydrogenase (*GAPDH*, used as internal reference; forward 5′-GGGCCAGAGACTGGCTCTTA-3′, reverse 5′-GATTCAGTGTGGTGGGGGAC-3′).

Western Blotting

Proteins were extracted using RIPA lysis buffer (P0013, Beyotime, Shanghai, China) containing phenylmethylsulfonyl fluoride (PMSF; ST505, Beyotime, Shanghai, China). BCA Kit (P0012, Beyotime, Shanghai, China) was used to quantify protein concentration. The protein samples were separated by sodium dodecyl sulfate (SDS)-polyacrylamide gel electrophoresis (10%; P0012A, Beyotime, Shanghai, China) and transferred onto polyvinylidene fluoride (PVDF) membranes (IPVH00010, Millipore, Billerica, MA, USA). After membranes were blocked with

5% nonfat milk at 37 °C for 1 h, they were incubated with primary antibodies targeting ZSWIM3 (1:1000 dilution; PA5-69969, Thermo Fisher Scientific, Waltham, MA, USA), SREBF1 (1:2000 dilution; ab313881), SREBF2 (1:2000 dilution; ab30682), acetyl-CoA carboxylase alpha (ACC1) (1:1000 dilution; ab45174), fatty acid synthase (FASN) (1:1000 dilution; ab128870), stearoyl-CoA desaturase (SCD1) (1:51000 dilution; ab19862), 3-hydroxy-3-methylglutaryl-CoA reductase (HMGCR) (1:1000 dilution; ab242315), 3-hydroxy-3-methylglutaryl-CoA synthase 1 (HMGCS1) (1:5000 dilution; ab155787), CD36 molecule (CD36) (1:1000 dilution; ab133625), carnitine palmitoyltransferase 1A (CPT1A) (1:1000 dilution; ab128568), acyl-CoA oxidase 1 (ACOX1) (1:1000 dilution; ab184032) and GAPDH (1:2000 dilution; ab8245) overnight at 4 °C. The membranes were then incubated with horseradish peroxidase-conjugated secondary antibodies (1:10000 dilution; ab6728 and ab205718). All antibodies except ZSWIM3 were purchased from Abcam (Cambridge, MA, USA). Subsequently, protein bands were visualized by means of enhanced chemiluminescence (ECL; WP20005, Invitrogen, Carlsbad, CA, USA) and were quantified by ImageJ software (1.48, National Institutes of Health, Rockville, MD, USA).

Quantification of Lipids

The cultured cells were treated with RIPA lysis buffer for 40 min. Lipids in the cells were subsequently isolated using chloroform (40007967, Sinopharm Chemical Reagent Co., Ltd., Shanghai, China) and mixed with methanol (10014108, Sinopharm Chemical Reagent Co., Ltd., Shanghai, China) at a ratio of 2:1. Using the commercially available assay kits purchased from Bioassay Systems (Hayward, CA, USA), the levels of cholesterol (ECCH-100), phospholipids (EPLP-100), triglyceride (ETGA-200), and free fatty acid (EFFA-200) were measured following the manufacturers' instructions.

Neutral Lipid Quantification

The cells were seeded on culture dishes and then fixed with 4% paraformaldehyde (P0099, Beyotime, Shanghai, China) for 15 min. Then, the cells were labeled by the BODIPY (1 µg/mL; C2053S, Beyotime, Shanghai, China) for 10–15 min in the dark. After rinsing the cells with phosphate-buffered saline (PBS; C0221A, Beyotime, Shanghai, China), the BODIPY staining results were analyzed by a flow cytometer (CytoFLEX, Beckman Coulter Inc., Brea, CA, USA).

Enzyme-Linked Immunosorbent Assay

The levels of a series of protein markers were determined using enzyme-linked immunosorbent assay (ELISA) kits in strict adherence with the manufacturers' instructions. The kits used include: SREBF1 (CSB-EL022657HU, CUSABIO, Wuhan, China), and SREBF2 (LS-F12655 LSBio, Shirley, MA, USA).

Cell Viability and Proliferation

Cell viability was determined by cell counting kit (CCK)-8 assay (G4103-1ML, Servicebio, Wuhan, China). Briefly, the cells were seeded into 96-well plates and cultured for 24 h. Each well contained 100 µL cell suspension with a concentration of 2.5×10^3 cells/mL. Then, CCK-8 solution (10 µL) was added to each well, and the cells were incubated for an additional 2 h. The absorbance was measured using the microplate reader (DR-200Bs, Diatek, Wuxi, China) at 450 nm.

Cell proliferation was determined by colony formation assay. Briefly, the cells were firstly digested by trypsin (T1300, Solarbio, Beijing, China) and then seeded into 24-well plates (1.5×10^3 cells/well). After being incubated for 14 days, the cells were fixed with 4% paraformaldehyde for 30 min and stained with 0.1% crystal violet dye (G1064, Solarbio, Beijing, China) for 30 min. Finally, the cell colonies formed were photographed by a camera (SLR, Nikon, Tokyo, Japan), and the number of colonies was analyzed using ImageJ software (1.48, National Institutes of Health, Rockville, MD, USA).

Cell Migration and Invasion

Cell migration and invasion were determined by Transwell assays using Transwell chamber (3422, Corning Inc., Corning, NY, USA). In the top chamber, 3×10^4 cells in 100 µL of FBS-free DMEM were added, whereas the bottom chamber was added with DMEM containing 20% FBS as a chemoattractant. The upper compartment with pre-coated Matrigel (0.2%; BD Biosciences, San Jose, CA, USA) was used for performing invasion assay, while the upper compartment without pre-coated Matrigel was used for conducting migration assay. After a 48-h incubation, the cells on the bottom surface were fixed with 4% paraformaldehyde for 15 min, stained with 0.5% crystal violet and counted under a microscope (CKX53, Olympus, Tokyo, Japan).

Statistical Analyses

Data are presented as mean ± standard deviation in this paper. GraphPad Prism 7.0 software (GraphPad Software Inc., San Diego, CA, USA) was employed for data analyses. Differences between groups were analyzed by the analysis of variance (ANOVA) followed by Tukey's post hoc tests. Differences were considered statistically significant at $p < 0.05$.

Results

ZSWIM3 Expression was Upregulated in BC Cells and Successfully Regulated via Transfection

Fig. 1A shows that the *ZSWIM3* mRNA was upregulated in BC cell lines compared to normal human mammary epithelial cells MCF10A ($p < 0.001$). The upregulation of *ZSWIM3* in BC cells was further verified by the

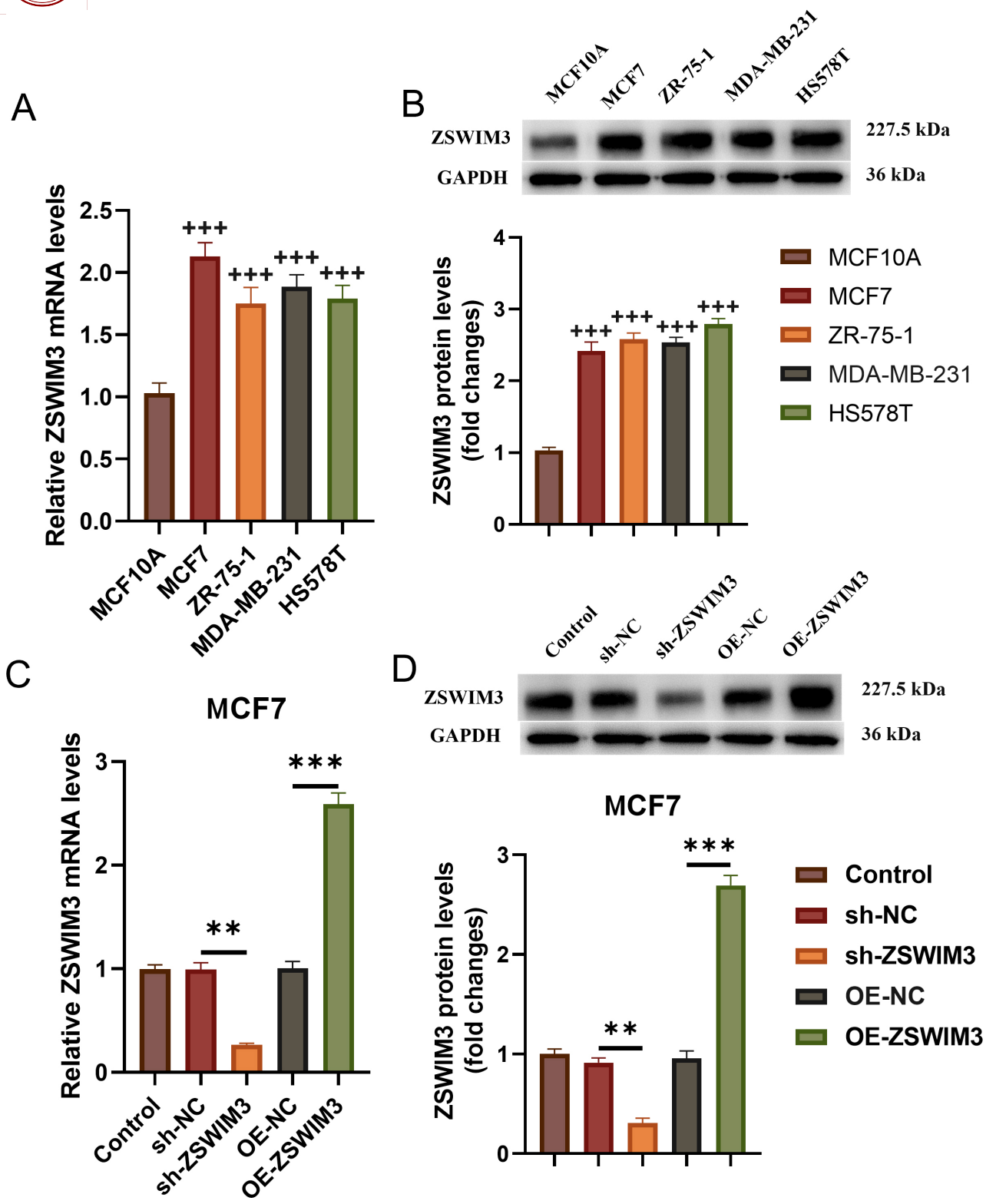

Fig. 1. *ZSWIM3* was upregulated in breast cancer (BC) cells and successfully regulated via transfection. (A,B) Levels of *ZSWIM3* mRNA (A) and protein (B) in normal human mammary epithelial MCF10A cells and BC cells. (C,D) Levels of *ZSWIM3* mRNA (C) and protein (D) in transfected MCF7 cells. n = 5. $^{+++}$ $p < 0.001$ compared with MCF10A; **$p < 0.01$, ***$p < 0.001$. *ZSWIM*, zinc-finger SWIM domain-containing protein family; *GAPDH*, glyceraldehyde-3-phosphate dehydrogenase; NC, negative control; sh, small hairpin.

Western blotting results, as shown in Fig. 1B, which show that the ZSWIM3 protein levels were remarkably higher in BC cell lines than in MCF10A ($p < 0.001$). Additionally, compared with sh-NC, sh-*ZSWIM3* significantly decreased the levels of *ZSWIM3* mRNA (Fig. 1C; $p < 0.01$) and protein (Fig. 1D; $p < 0.01$), whereas compared with

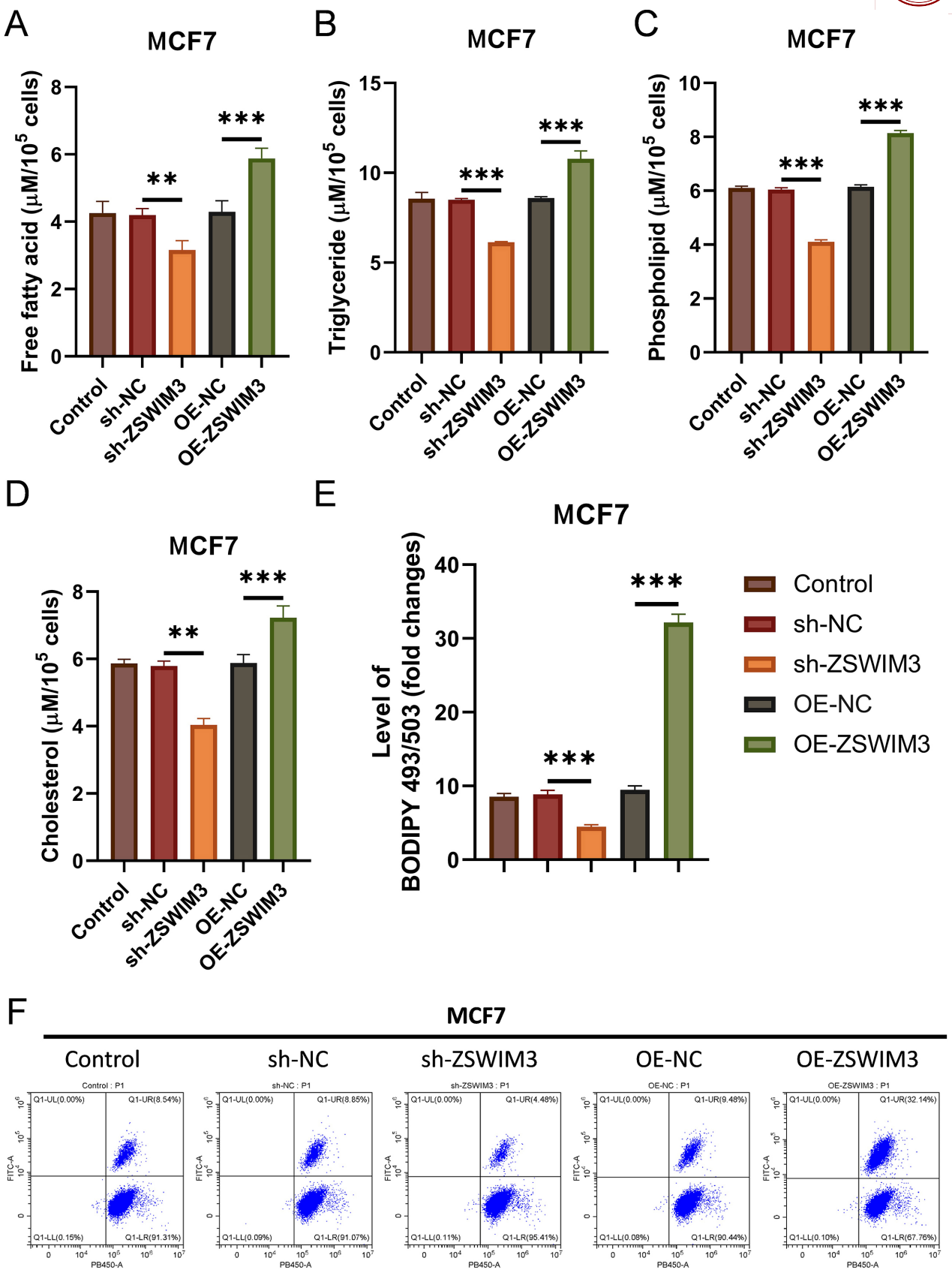

Fig. 2. *ZSWIM3* increased lipid contents in BC cells. (A–D) Levels of free fatty acid (A), triglyceride (B), phospholipids (C) and cholesterol (D) in transfected MCF7 cells. (E,F) Quantification of BODIPY level (E) and representative flow cytometry results of BODIPY staining (F). n = 5. $^{**}p < 0.01$, $^{***}p < 0.001$.

OE-NC, OE-*ZSWIM3* significantly increased the levels of *ZSWIM3* mRNA (Fig. 1C; $p < 0.001$) and protein (Fig. 1D; $p < 0.001$), suggesting that the *ZSWIM3* expression can be manipulated through transfection means.

ZSWIM3 Increased Lipid Contents in BC Cells

As shown in Fig. 2A–D, intracellular free fatty acid (Fig. 2A), triglyceride (Fig. 2B), phospholipids (Fig. 2C) and cholesterol (Fig. 2D) were decreased significantly in sh-*ZSWIM3*-transfected MCF7 cells, as compared with sh-NC-transfected MCF7 cells ($p < 0.01$), but were elevated significantly in OE-*ZSWIM3*-transfected MCF7 cells when compared with OE-NC-transfected MCF7 cells ($p < 0.001$). Moreover, the level of BODIPY (Fig. 2E,F), which reflects the level of intracellular neutral lipids staining, was remarkably lower in sh-*ZSWIM3*-transfected MCF7 cells than in their sh-NC-transfected counterparts ($p < 0.001$), whereas OE-*ZSWIM3* transfection resulted in remarkably higher BODIPY level compared to the OE-NC-transfected MCF7 cells ($p < 0.001$). All these findings indicated that the *ZSWIM3* increased levels of lipid contents in BC cells, playing a regulatory role in the lipid metabolism of BC cells.

ZSWIM3 Promoted the Expression of Lipogenic Enzymes in BC Cells

The expression of fatty acid synthesis-related markers such as ACC1 (Fig. 3A,B), FASN (Fig. 3A,C) and SCD1 (Fig. 3A,D) was suppressed in *ZSWIM3*-knockdown BC cells ($p < 0.01$) but promoted in *ZSWIM3*-overexpressing BC cells ($p < 0.001$). Moreover, the levels of cholesterol biosynthesis-related HMGCR (Fig. 3A,E) and HMGCS1 (Fig. 3A,F) were decreased in the sh-*ZSWIM3* group relative to in the sh-NC group ($p < 0.01$). As compared to OE-NC goup, however, OE-*ZSWIM3* group exhibited increased level of HMGCR ($p < 0.001$). Furthermore, as shown in Fig. 3G–I, the alterations of *ZSWIM3* expression did not affect the levels of fatty acid uptake-related factor CD36 (Fig. 3A,G) and fatty acid oxidation-related factors CPT1A (Fig. 3A,H) and ACOX1 (Fig. 3A,I). Taken together, these results indicated that *ZSWIM3* regulated lipid metabolism mainly by promoting lipogenesis.

ZSWIM3 Knockdown Decreased Lipid Contents in BC Cell by Downregulating SREBF1/SREBF2

The sh-*ZSWIM3* transfection decreased *SREBF1* mRNA (Fig. 4A) and protein levels (Fig. 4B,C) in BC cells ($p < 0.01$, sh-*ZSWIM3* vs. sh-NC), which could be restored by OE-*SREBF1* transfection ($p < 0.01$, sh-*ZSWIM3*+OE-*SREBF1* vs. sh-*ZSWIM3*+OE-NC). Similarly, the sh-*ZSWIM3* transfection reduced *SREBF2* protein and mRNA levels (Fig. 4D–F) in BC cells ($p < 0.01$ sh-*ZSWIM3* vs. sh-NC), which could be reversed by OE-*SREBF2* transfection ($p < 0.01$, sh-*ZSWIM3*+OE-*SREBF2* vs. sh-*ZSWIM3*+OE-NC). OE-*SREBF1* transfection could reverse the *ZSWIM3* knockdown-induced reductions of free fatty acid (Fig. 4G), triglyceride (Fig. 4H) and phospholipids (Fig. 4I) by upregulating *SREBF1* expression ($p < 0.001$). Similarly, the *ZSWIM3* knockdown-induced decrease of cholesterol (Fig. 4J) was restored when *SREBF2* expression was upregulated as a result of OE-*SREBF2* transfection ($p < 0.001$). Accordingly, the *ZSWIM3* knockdown decreased the lipid contents in BC cells only when the *SREBF1/SREBF2* was downregulated.

ZSWIM3 Knockdown Suppressed BC Cell Growth and Metastasis by Decreasing Lipid Biosynthesis

The cell viability (Fig. 5A) was lower in the sh-*ZSWIM3* group than in the sh-NC group ($p < 0.001$), which was reversed by the *SREBF1/SREBF2* overexpression ($p < 0.001$). This observation indicates that *ZSWIM3* knockdown can suppress BC cell viability by suppressing lipid synthesis through the downregulation of *SREBF1/SREBF2*. Moreover, Fig. 5B,C shows that the cell migration and invasion were decreased in the sh-*ZSWIM3* group, as compared with sh-NC group ($p < 0.001$). Similarly, overexpression of *SREBF1/SREBF2* could reverse the lowered migration ability and invasiveness of BC cells ($p < 0.001$), indicating that suppressing lipid synthesis is the principal mechanism of inhibiting BC cell metastasis in the context of *ZSWIM3* knockdown.

ZSWIM3 Overexpression Increased Lipid Contents in BC Cell by Upregulating SREBF1/SREBF2

The OE-*ZSWIM3* significantly increased *SREBF1* mRNA (Fig. 6A) and protein levels (Fig. 6B) in BC cells ($p < 0.001$, OE-*ZSWIM3* vs. OE-NC), and such elevations were reversible through sh-*SREBF1* transfection ($p < 0.001$, OE-*ZSWIM3*+sh-*SREBF1* vs. OE-*ZSWIM3*+sh-NC). The *ZSWIM3* overexpression-induced spike of free fatty acid (Fig. 6C), triglyceride (Fig. 6D) and phospholipids levels (Fig. 6E) were reversed when *SREBF1* expression was downregulated by sh-*SREBF1* ($p < 0.001$). Similarly, the increase in *SREBF2* mRNA (Fig. 6F) and protein levels (Fig. 6G) in BC cells as a result of OE-*ZSWIM3* transfection ($p < 0.001$, OE-*ZSWIM3* vs. OE-NC) could be reversed by sh-*SREBF2* transfection ($p < 0.001$, OE-*ZSWIM3*+sh-*SREBF2* vs. OE-*ZSWIM3*+sh-NC). It was also found that the knockdown of *SREBF2* by sh-*SREBF2* transfection can reverse the *ZSWIM3* overexpression-induced increase of cholesterol (Fig. 6H; $p < 0.001$). Thus, these findings highlighted that the increased levels of lipid contents in BC cells during the *ZSWIM3* overexpression were mediated through the *SREBF1/SREBF2* upregulation.

ZSWIM3 Overexpression Promoted BC Cell Growth and Metastasis by Increasing Lipid Biosynthesis

In this study, we found that the *ZSWIM3* overexpression promoted BC cell viability through *SREBF1/SREBF2*

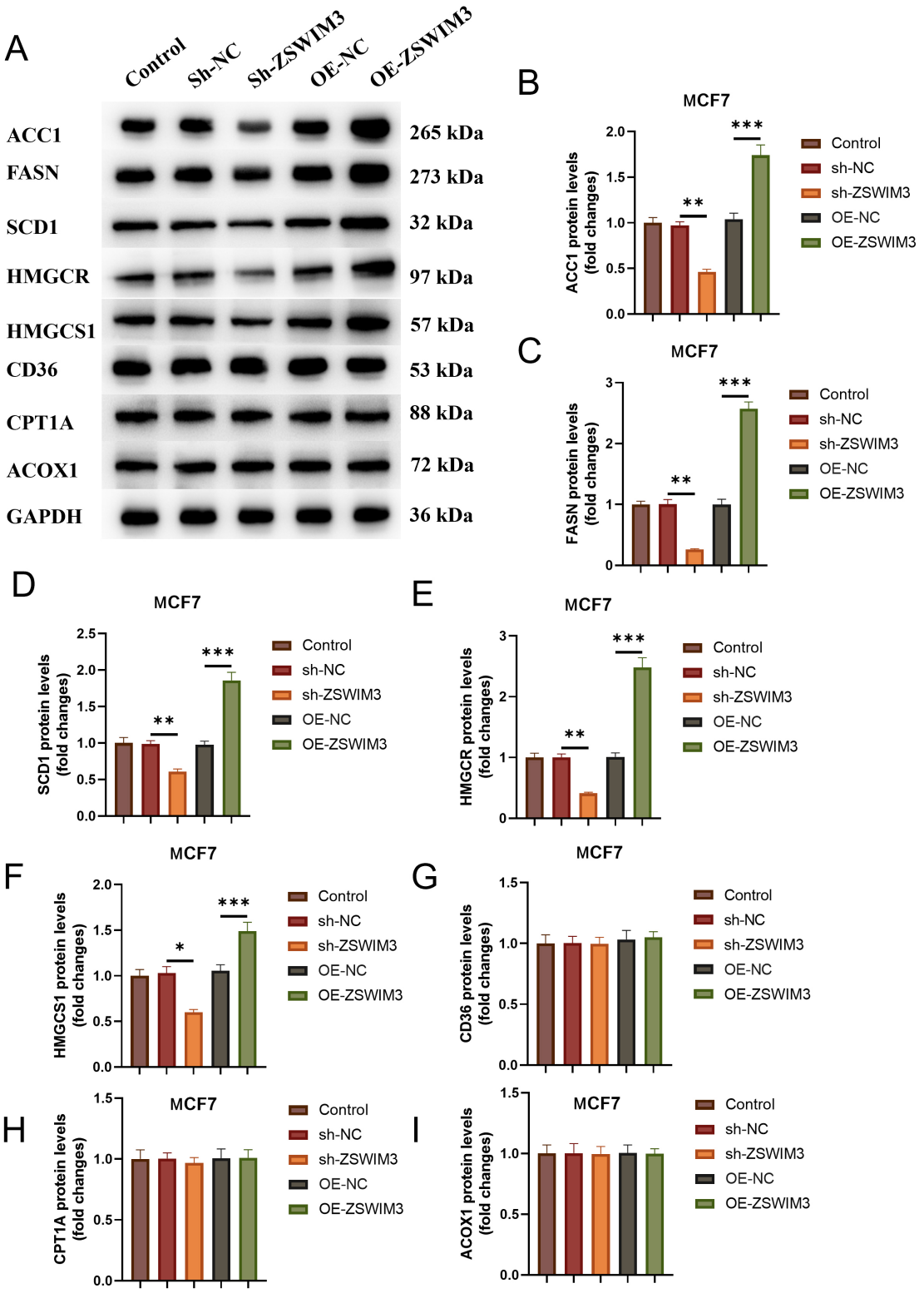

Fig. 3. *ZSWIM3* promoted the expression of lipogenic enzymes in BC cells. (A) Western blotting results depict protein expression levels of various lipogenic enzymes. (B–I) Quantification of protein levels of lipogenic enzymes in transfected cells based on Western blotting results: acetyl-CoA carboxylase alpha (ACC1; B), fatty acid synthase (FASN; C), stearoyl-CoA desaturase (SCD1; D), 3-hydroxy-3-methylglutaryl-CoA reductase (HMGCR; E), 3-hydroxy-3-methylglutaryl-CoA synthase 1 (HMGCS1; F); CD36 molecule (CD36; G), carnitine palmitoyltransferase 1A (CPT1A; H), and acyl-CoA oxidase 1 (ACOX1; I). n = 5. *$p < 0.05$, **$p < 0.01$, ***$p < 0.001$.

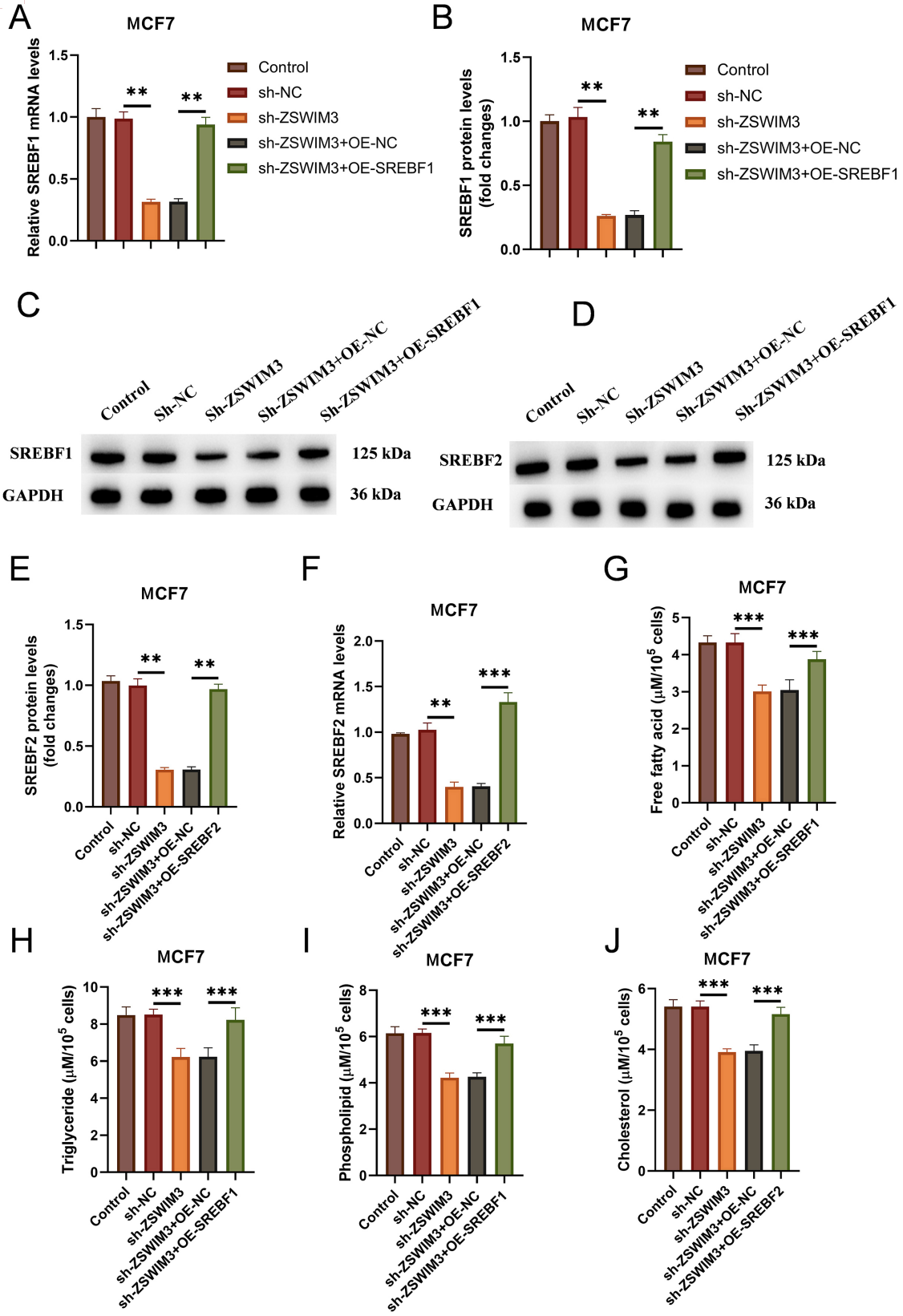

Fig. 4. *ZSWIM3* knockdown decreased lipid contents in BC cells by downregulating *SREBF1/SREBF2*. (A–C) *SREBF1* mRNA (A) and protein levels (B,C) in transfected MCF7 cells. (D–F) *SREBF2* protein (D,E) and mRNA (F) in transfected MCF7 cells. (G–I) Levels of free fatty acid (G), triglyceride (H) and phospholipids (I). (J) Levels of cholesterol. n = 5. $^{**}p < 0.01$, $^{***}p < 0.001$. SREBF1, sterol regulatory element-binding transcription factor 1.

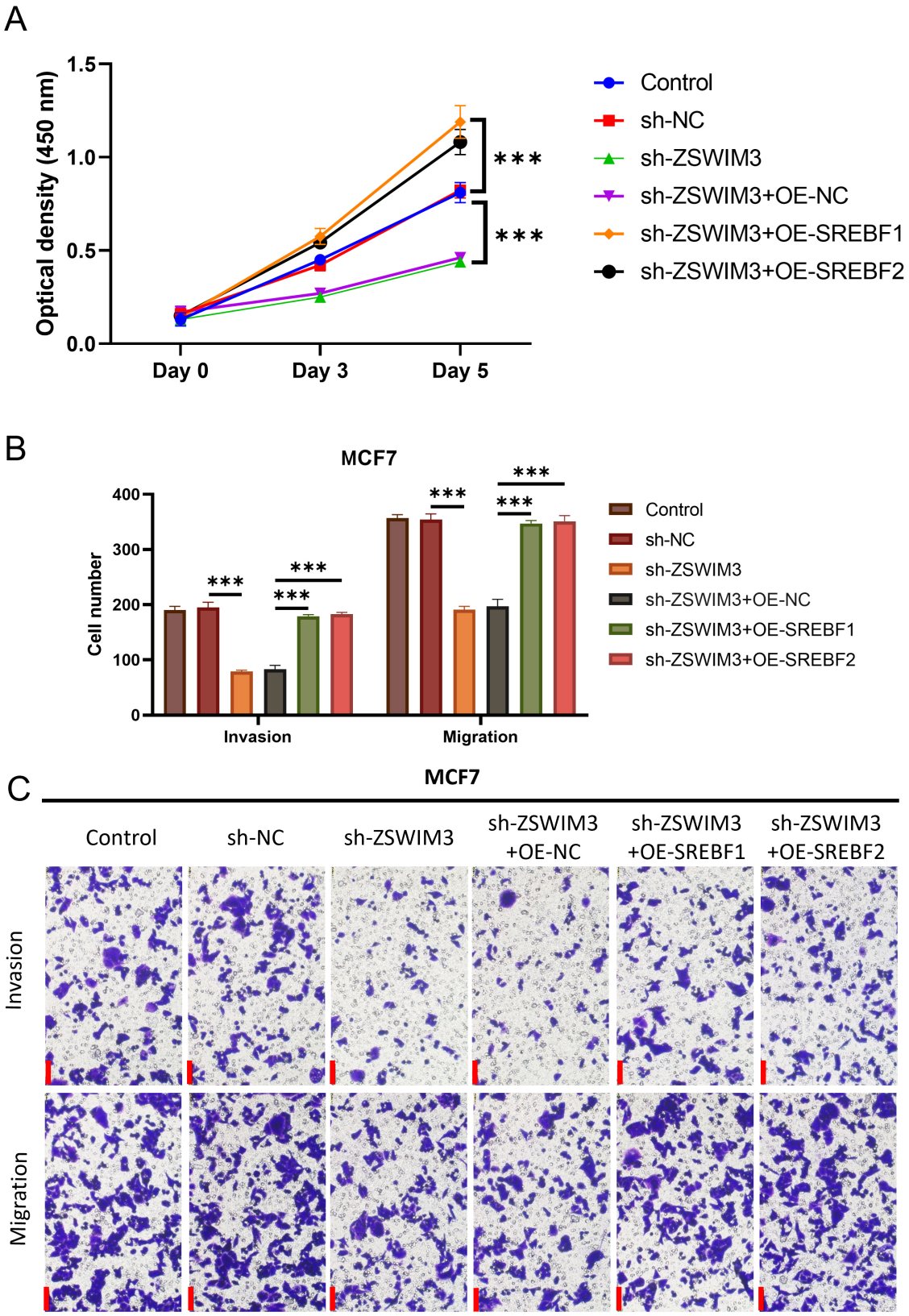

Fig. 5. *ZSWIM3* knockdown suppressed BC cell growth and metastasis by decreasing lipid biosynthesis. (A) Cell counting kit (CCK)-8 assay results. (B,C) Transwell assay results for determining migration and invasion of BC cells (scale bar: 50 μm). n = 5. ***$p < 0.001$.

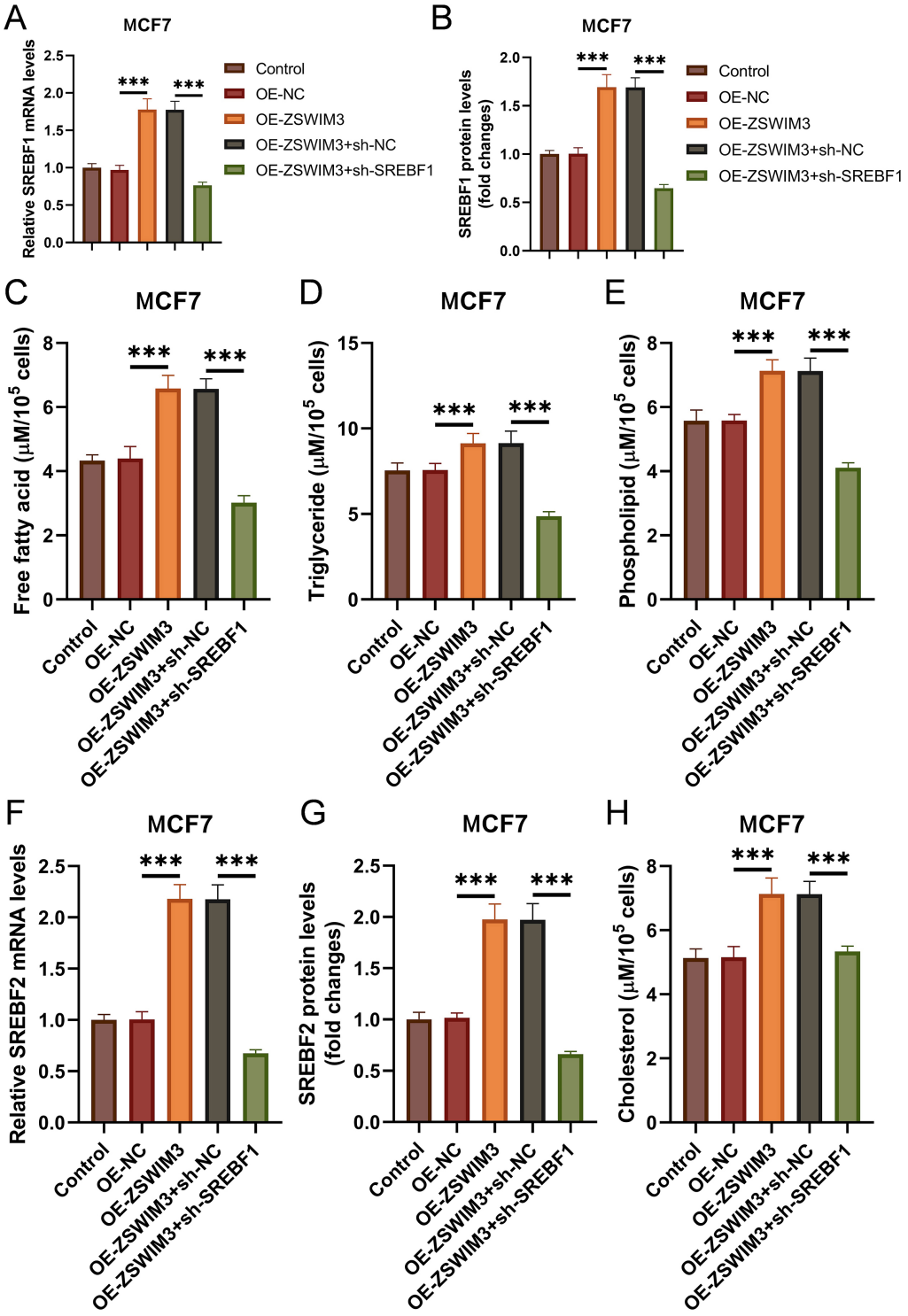

Fig. 6. *ZSWIM3* overexpression increased lipid contents in BC cell by upregulating *SREBF1/SREBF2*. (A,B) *SREBF1* mRNA (A) and protein levels (B) in transfected MCF7 cells were determined by Real-Time Reverse-Transcription Polymerase Chain Reaction (RT-qPCR) and enzyme-linked immunosorbent assay (ELISA). (C–E) Levels of free fatty acid (C), triglyceride (D) and phospholipids (E) in transfected MCF7 cells. (F,G) *SREBF2* mRNA (F) and protein levels (G) in transfected MCF7 cells were determined by RT-qPCR and ELISA. (H) Cholesterol levels in transfected MCF7 cells. n = 5. ***$p < 0.001$.

upregulation, which can be translated to augmented lipid synthesis. This postulation is supported by the current finding that the increased cell viability in the OE-*ZSWIM3* group, relative to that in the OE-NC group ($p < 0.001$; Fig. 7A), could be reversed by downregulating *SREBF1/SREBF2* ($p < 0.001$). Moreover, compared to the OE-NC group, the OE-*ZSWIM3* group displayed enhanced cell migration and invasion ($p < 0.001$; Fig. 7B,C), which

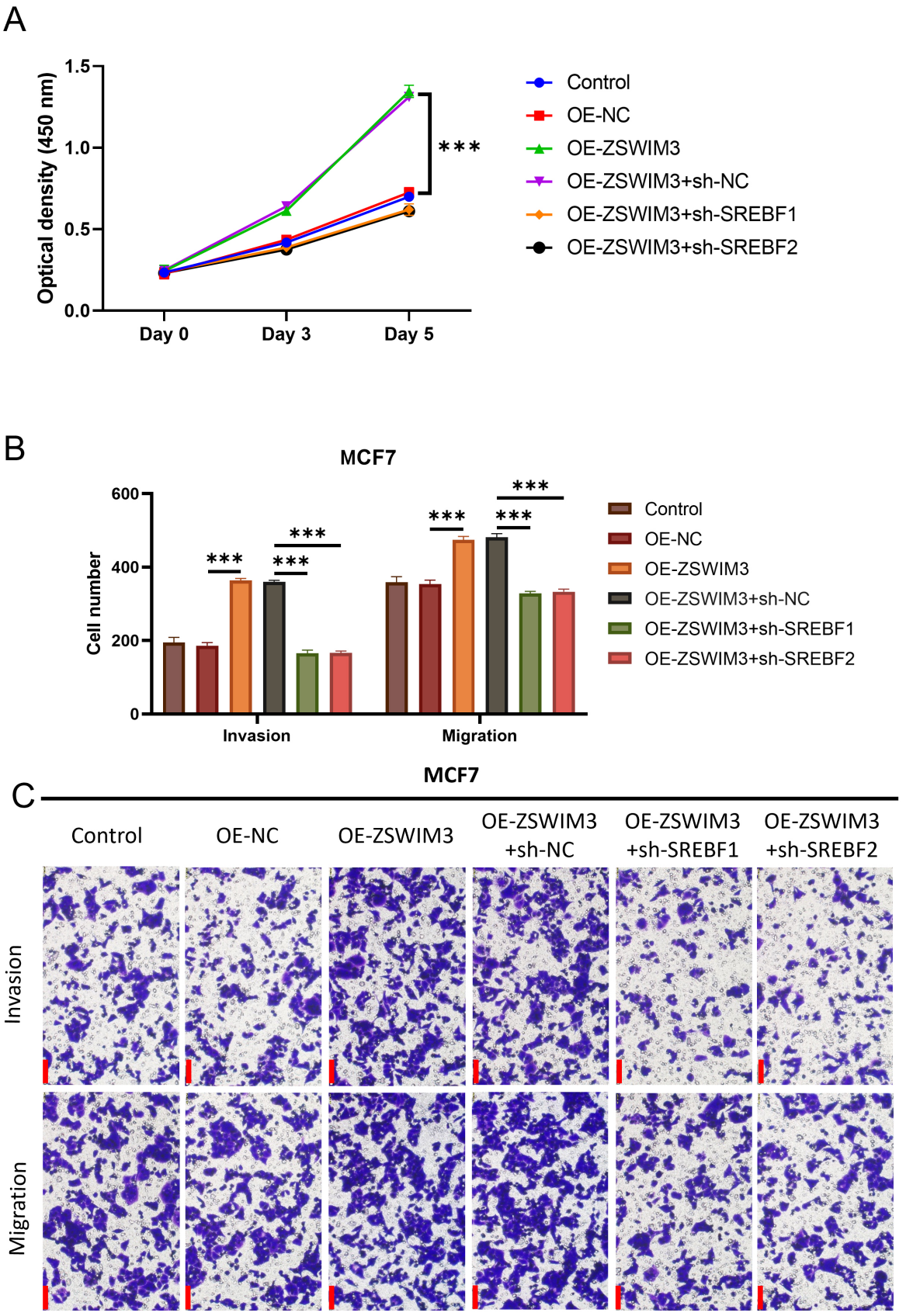

Fig. 7. ZSWIM3 overexpression promoted BC cell growth and metastasis by increasing lipid biosynthesis. (A) CCK-8 assay results. (B,C) Transwell assay results for migration and invasion determination (scale bar: 50 μm). n = 5. ***$p < 0.001$.

were reversible by *SREBF1/SREBF2* downregulation ($p < 0.001$), indicating that *ZSWIM3* overexpression promoted BC cell metastasis by increasing lipid synthesis.

Discussion

In this study, we demonstrated that *ZSWIM3* promotes lipid synthesis in BC cells by upregulating *SREBP1*, *SREBP2*, and their target enzymes, consequently contributing to the proliferation and metastasis of BC cells. The current set of findings lend support to the theory that *ZSWIM3* and the lipid metabolism reprogramming mediated by *ZSWIM3* play critical roles in BC progression.

The elevated *de novo* synthesis of fatty acid in various types of cancers is considered a major pathway by which cancer cells acquire fatty acid [7]. Studies have also shown that genes that encode critical lipogenesis regulators are upregulated in cancers [23,24]. Moreover, some of these lipogenesis regulators play direct roles in cancer development and progression. For instance, ACC1 is involved in the metastasis and recurrence of BC [25], and the inhibition of ACC1 could reduce BC cell viability and suppress BC progression both *in vitro* and *in vivo* [26]. Additionally, FASN [27,28] and SCD1 [29,30] are associated with the accelerated progression and malignancy of BC. Consistently, our results demonstrated that the *ZSWIM3* is responsible for the viability, proliferation and metastasis of BC cells by augmenting the levels of ACC1, FASN and SCD1.

Furthermore, increased levels of intracellular cholesterol are frequently detected in many types of cancers [31,32], and thus, reprogramming cholesterol metabolism is touted as a potential anticancer strategy [33]. For example, both HMGCR and HMGCS1—the rate-limiting enzymes during cholesterol biosynthesis—participate in the progression of cancers. The inhibition of these two enzymes suppresses the mevalonate pathway, leading to suppressed tumor cell growth and boosted antitumor immunity [34]. HMGCR has been proven to be the driver and a therapeutic target of liver cancer [35], lung cancer [36], prostate cancer [37], etc. In this study, we discovered that both HMGCR and HMGCS1, aside from engaging in cholesterol synthesis, played crucial roles in BC cell progression under the regulation of *ZSWIM3*.

SREBPs are central transcriptional factors for controlling lipid synthesis and exerting regulatory effects on cancers. Among the different members of SREBPs, SREBP1 and SREBP2 have specific roles in regulating fatty acid synthesis and cholesterol synthesis, respectively [38,39]. A growing body of studies has illuminated the unexpected functions of the SREBPs as therapeutic targets for cancers, including BC [40–42]. In this study, we demonstrated that ZSWIM3 increased *SREBP1* and *SREBP2* expression in BC cells, further proving that the fatty acid synthesis mediated by *SREBP1* and the cholesterol synthesis governed by *SREBP2* play crucial roles in BC progression. Moreover, we found that the knockdown of *SREBP1* or *SREBP2* attenuated or even offset the *ZSWIM3* overexpression-driven BC cell progression, proving the significance of dysregulated lipid metabolism in BC progression. These findings offer a preliminary picture that *ZSWIM3* promotes BC progression by regulating lipid metabolism, establishing *ZSWIM3* and other lipid markers as potential therapeutic targets for BC.

This study primarily utilized the MCF7 cell line to investigate the role of *ZSWIM3* in BC progression. Although MCF7 cells are widely used in BC research, their characteristics may not fully represent the heterogeneity of BC. Future studies could incorporate other BC cell lines to validate the research results and ensure their generalizability. *In vitro* cell culture experiments were heavily relied upon in the study to assess the impact of *ZSWIM3* on lipid metabolism and BC progression. While *in vitro* models provide invaluable insights, they may not fully replicate the complexity of the tumor microenvironment *in vivo*. Future research could exploit the use of animal models or patient-derived xenografts to validate the observed effects in a more physiologically relevant environment. Another shortcoming of this study is the mere elucidation of the effects of *ZSWIM3* on lipid metabolism regulation and BC progression, without delving deeply into the precise molecular mechanisms underlying these effects. Future mechanistic studies, with a focus on elucidating downstream signaling pathways and protein interactions, should be conducted to complete our understanding of the role played by *ZSWIM3* in BC pathogenesis. Another direction along which future research can exploit for validation purposes is to explore the clinical relevance of *ZSWIM3* expression levels in humans' diseased samples with BC progression. Correlating *ZSWIM3* expression with clinicopathological features and patient outcomes could provide useful insights into its prognostic significance and validate its potential as a therapeutic target. Considering the role of *ZSWIM3* in promoting lipid synthesis and breast cancer progression, developing drugs to target *ZSWIM3* or its downstream effectors may be a promising avenue. Given the multifaceted nature of BC progression, combination therapies targeting multiple pathways, including lipid metabolism and other key signaling cascades, may lead to more effective treatment outcomes. Future studies could explore the synergistic interactions between *ZSWIM3* inhibitors and the existing anticancer drugs to develop more effective treatment regimens.

Knockout or overexpression of *ZSWIM3* may affect lipid metabolism within cells, leading to an increase or decrease in lipid synthesis and storage. This could further influence cell growth, proliferation, and metastatic ability, thus affecting tumor development and progression. Long-term knockout of *ZSWIM3* may suppress the growth and metastatic ability of BC cells, thereby slowing down tumor progression. Conversely, overexpression of *ZSWIM3* may promote the growth and metastasis of BC cells, accelerating tumor progression. Based on these findings, longstanding *ZSWIM3* knockout may have a positive impact on patient health, potentially reducing the tumor burden and risk

of disease progression in BC patients. However, overexpression of *ZSWIM3* may increase the tumor burden and risk of disease progression, thus negatively affecting patient health. Thus, regulating *ZSWIM3* expression to inhibit tumor development and progression is a potential therapeutic avenue in BC treatment. Despite the significant effects on cell activities and lipid contents, the specific impacts of *ZSWIM3* on BC development need to be further unraveled to identify new regulatory mechanisms involving *ZSWIM3* underlying BC progression.

Conclusion

In conclusion, the *ZSWIM3* plays a role in accelerating BC progression by augmenting lipid biosynthesis. The findings in this study provide preliminary evidence of the effect of *ZSWIM3* on BC progression, as well as the involvement of reprogrammed lipid metabolism as the mediator of enhanced cancer cell proliferation and metastasis as a consequence of *ZSWIM3* upregulation. This study also offers some new insights into establishing the molecular mechanism involving *ZSWIM3* and other related lipogenic proteins as therapeutic targets for BC treatment.

Availability of Data and Materials

Data to support the findings of this study are available on reasonable request from the corresponding authors.

Author Contributions

XM and ACW designed the research study. YW, JTM and YM performed the research. YCL and YM provided help and advice on the ELISA experiments and analyzed the data. YM and XM wrote the first draft. All authors contributed significantly to editorial changes of important content. All authors read and approved the final manuscript. All authors have participated sufficiently in the work and agreed to be accountable for all aspects of the work.

Ethics Approval and Consent to Participate

Not applicable.

Acknowledgment

Not applicable.

Funding

This research was funded by the 2022 Jinan Municipal Health Commission Science and Technology Plan Project, Grant No. 2022-2-112.

Conflict of Interest

The authors declare no conflict of interest.

References

[1] Sung H, Ferlay J, Siegel RL, Laversanne M, Soerjomataram I, Jemal A, *et al*. Global Cancer Statistics 2020: GLOBOCAN Estimates of Incidence and Mortality Worldwide for 36 Cancers in 185 Countries. CA: A Cancer Journal for Clinicians. 2021; 71: 209–249.

[2] Momenimovahed Z, Salehiniya H. Epidemiological characteristics of and risk factors for breast cancer in the world. Breast Cancer (Dove Medical Press). 2019; 11: 151–164.

[3] Ben-Dror J, Shalamov M, Sonnenblick A. The History of Early Breast Cancer Treatment. Genes. 2022; 13: 960.

[4] Nassif AB, Talib MA, Nasir Q, Afadar Y, Elgendy O. Breast cancer detection using artificial intelligence techniques: A systematic literature review. Artificial Intelligence in Medicine. 2022; 127: 102276.

[5] Kawiak A. Molecular Research and Treatment of Breast Cancer. International Journal of Molecular Sciences. 2022; 23: 9617.

[6] Liu S, Sun Y, Hou Y, Yang L, Wan X, Qin Y, *et al*. A novel lncRNA ROPM-mediated lipid metabolism governs breast cancer stem cell properties. Journal of Hematology & Oncology. 2021; 14: 178.

[7] Jin Z, Chai YD, Hu S. Fatty Acid Metabolism and Cancer. Advances in Experimental Medicine and Biology. 2021; 1280: 231–241.

[8] Koundouros N, Poulogiannis G. Reprogramming of fatty acid metabolism in cancer. British Journal of Cancer. 2020; 122: 4–22.

[9] King RJ, Singh PK, Mehla K. The cholesterol pathway: impact on immunity and cancer. Trends in Immunology. 2022; 43: 78–92.

[10] Xu H, Zhou S, Tang Q, Xia H, Bi F. Cholesterol metabolism: New functions and therapeutic approaches in cancer. Biochimica et Biophysica Acta. Reviews on Cancer. 2020; 1874: 188394.

[11] Zipinotti Dos Santos D, de Souza JC, Pimenta TM, da Silva Martins B, Junior RSR, Butzene SMS, *et al*. The impact of lipid metabolism on breast cancer: a review about its role in tumorigenesis and immune escape. Cell Communication and Signaling. 2023; 21: 161.

[12] Xie Y, Wang B, Zhao Y, Tao Z, Wang Y, Chen G, *et al*. Mammary adipocytes protect triple-negative breast cancer cells from ferroptosis. Journal of Hematology & Oncology. 2022; 15: 72.

[13] Rakhra G, Rakhra G. Zinc finger proteins: insights into the transcriptional and post transcriptional regulation of immune response. Molecular Biology Reports. 2021; 48: 5735–5743.

[14] Zhao J, Wen D, Zhang S, Jiang H, Di X. The role of zinc finger proteins in malignant tumors. FASEB Journal. 2023; 37: e23157.

[15] Hassan IU, Rehman HM, Liu Z, Zhou L, Samma MK, Wang C, *et al*. Genome-wide identification and spatiotemporal expression profiling of zinc finger SWIM domain-containing protein family genes. Zoological Research. 2023; 44: 663–674.

[16] He J, Wu M, Xiong L, Gong Y, Yu R, Peng W, *et al*. BTB/POZ zinc finger protein ZBTB16 inhibits breast cancer proliferation and metastasis through upregulating ZBTB28 and antagonizing BCL6/ZBTB27. Clinical Epigenetics. 2020; 12: 82.

[17] Wu X, Zhang X, Yu L, Zhang C, Ye L, Ren D, *et al*. Zinc finger protein 367 promotes metastasis by inhibiting the Hippo pathway in breast cancer. Oncogene. 2020; 39: 2568–2582.

[18] An G, Feng L, Hou L, Li X, Bai J, He L, *et al*. A bioinformatics analysis of zinc finger protein family reveals potential oncogenic biomarkers in breast cancer. Gene. 2022; 828: 146471.

[19] Li HD, Chen X, Xu JJ, Du XS, Yang Y, Li JJ, *et al*. DNMT3b-mediated methylation of ZSWIM3 enhances inflammation in alcohol-induced liver injury via regulating TRAF2-mediated NF-κB pathway. Clinical Science. 2020; 134: 1935–1956.

[20] Broadfield LA, Pane AA, Talebi A, Swinnen JV, Fendt SM. Lipid metabolism in cancer: New perspectives and emerging mechanisms. Developmental Cell. 2021; 56: 1363–1393.

[21] Wu M, Yang Z, Zhang C, Shi Y, Han W, Song S, *et al*. Inhibition of NLRP3 inflammasome ameliorates podocyte damage by suppressing lipid accumulation in diabetic nephropathy. Metabolism: Clinical and Experimental. 2021; 118: 154748.

[22] Bengoechea-Alonso MT, Aldaalis A, Ericsson J. Loss of the Fbw7 tumor suppressor rewires cholesterol metabolism in cancer cells leading to activation of the PI3K-AKT signalling axis. Frontiers in Oncology. 2022; 12: 990672.

[23] Chen L, Duan Y, Wei H, Ning H, Bi C, Zhao Y, *et al*. Acetyl-CoA carboxylase (ACC) as a therapeutic target for metabolic syndrome and recent developments in ACC1/2 inhibitors. Expert Opinion on Investigational Drugs. 2019; 28: 917–930.

[24] Tracz-Gaszewska Z, Dobrzyn P. Stearoyl-CoA Desaturase 1 as a Therapeutic Target for the Treatment of Cancer. Cancers. 2019; 11: 948.

[25] Rios Garcia M, Steinbauer B, Srivastava K, Singhal M, Mattijssen F, Maida A, *et al*. Acetyl-CoA Carboxylase 1-Dependent Protein Acetylation Controls Breast Cancer Metastasis and Recurrence. Cell Metabolism. 2017; 26: 842–855.e5.

[26] Marczyk M, Gunasekharan V, Casadevall D, Qing T, Foldi J, Sehgal R, *et al*. Comprehensive Analysis of Metabolic Isozyme Targets in Cancer. Cancer Research. 2022; 82: 1698–1711.

[27] Chaturvedi S, Biswas M, Sadhukhan S, Sonawane A. Role of EGFR and FASN in breast cancer progression. Journal of Cell Communication and Signaling. 2023; 17: 1249–1282.

[28] Huang X, Tan W, Liu Z, Fu X, Li Z, Lai S, *et al*. EIF4A3-induced circZFAND6 promotes breast cancer proliferation and metastasis through the miR-647/FASN axis. Life Sciences. 2023; 324: 121745.

[29] Chen J, Lv S, Huang B, Ma X, Fu S, Zhao Y. Upregulation of SCD1 by ErbB2 via LDHA promotes breast cancer cell migration and invasion. Medical Oncology. 2022; 40: 40.

[30] Luis G, Godfroid A, Nishiumi S, Cimino J, Blacher S, Maquoi E, *et al*. Tumor resistance to ferroptosis driven by Stearoyl-CoA Desaturase-1 (SCD1) in cancer cells and Fatty Acid Biding Protein-4 (FABP4) in tumor microenvironment promote tumor recurrence. Redox Biology. 2021; 43: 102006.

[31] Huang B, Song BL, Xu C. Cholesterol metabolism in cancer: mechanisms and therapeutic opportunities. Nature Metabolism. 2020; 2: 132–141.

[32] Kopecka J, Trouillas P, Gašparović AČ, Gazzano E, Assaraf YG, Riganti C. Phospholipids and cholesterol: Inducers of cancer multidrug resistance and therapeutic targets. Drug Resistance Updates. 2020; 49: 100670.

[33] Ediriweera MK. Use of cholesterol metabolism for anti-cancer strategies. Drug Discovery Today. 2022; 27: 103347.

[34] Zhou W, Liu H, Yuan Z, Zundell J, Towers M, Lin J, *et al*. Targeting the mevalonate pathway suppresses ARID1A-inactivated cancers by promoting pyroptosis. Cancer Cell. 2023; 41: 740–756.e10.

[35] Alannan M, Trézéguet V, Amoêdo ND, Rossignol R, Mahfouf W, Rezvani HR, *et al*. Rewiring Lipid Metabolism by Targeting PCSK9 and HMGCR to Treat Liver Cancer. Cancers. 2022; 15: 3.

[36] Yuan H, Wu H, Cheng J, Xiong J. SIAH1 ubiquitination-modified HMGCR inhibits lung cancer progression and promotes drug sensitivity through cholesterol synthesis. Cancer Cell International. 2023; 23: 71.

[37] Basavaraj P, Ruangsai P, Hsieh PF, Jiang WP, Bau DT, Huang GJ, *et al*. Alpinumisoflavone Exhibits the Therapeutic Effect on Prostate Cancer Cells by Repressing AR and Co-Targeting FASN- and HMGCR-Mediated Lipid and Cholesterol Biosynthesis. Life. 2022; 12: 1769.

[38] Zhao Q, Lin X, Wang G. Targeting SREBP-1-Mediated Lipogenesis as Potential Strategies for Cancer. Frontiers in Oncology. 2022; 12: 952371.

[39] Xue L, Qi H, Zhang H, Ding L, Huang Q, Zhao D, *et al*. Targeting SREBP-2-Regulated Mevalonate Metabolism for Cancer Therapy. Frontiers in Oncology. 2020; 10: 1510.

[40] Chen YY, Ge JY, Zhu SY, Shao ZM, Yu KD. Copy number amplification of ENSA promotes the progression of triple-negative breast cancer via cholesterol biosynthesis. Nature Communications. 2022; 13: 791.

[41] Hwang HJ, Lee KH, Cho JY. ABCA9, an ER cholesterol transporter, inhibits breast cancer cell proliferation via SREBP-2 signaling. Cancer Science. 2023; 114: 1451–1463.

[42] Pham DV, Tilija Pun N, Park PH. Autophagy activation and SREBP-1 induction contribute to fatty acid metabolic reprogramming by leptin in breast cancer cells. Molecular Oncology. 2021; 15: 657–678.